

A Discussion on Design Fires for an Example High-Speed Railway Train Car

W.C. Xiao¹, W.K. Chow^{1*} and W. Peng²

0000-0001-7750-8054, 0000-0001-8398-3126, 0000-0002-8451-7693

¹ Department of Building Environment and Energy Engineering, The Hong Kong Polytechnic University, Hong Kong, China

² School of Energy and Safety, Anhui University of Science and Technology, Anhui, China

Abstract

High-speed rail systems are expanding everywhere for carrying thousands of passengers every day. Train cars in underground spaces travel under dense urban areas, tunnels in mountainous places and bridges across rivers. Design fire in burning a train car should be studied carefully for fire hazard assessment in those long underground or enclosed spaces. There are full-scale burning testing results on the main combustibles including seat, curtain and passenger luggage in some train cars. The heat release rate of a high-speed train car model CRH1 will be studied using such data together with a two-layer fire zone model, the Consolidated Model of Fire and Smoke Transport (CFAST). Simulation will be performed on the full-sized train car with the heat release rate of the seat measured by experiment. Two fire scenarios with ignition points located in the front and rear areas of the train compartment are considered. The results of the fire simulations show that the heat release rate can reach 43 MW. The value is similar to the full-scale burning experiments on train cars in Sweden and South Korea. Active fire protection systems have to be seriously considered in those underground or enclosed areas.

Keywords: High-speed railway, Train car fires; Fire hazard assessment; Design fires.

Research Article

<https://doi.org/10.30939/ijastech..1058890>

Received 15.02.2022
Revised 08.04.2022
Accepted 29.04.2022

* Corresponding author

W.K. Chow

wan-ki.chow@polyu.edu.hk

Address: The Hong Kong Polytechnic University, Hong Kong, China

Tel:+85227665843

1. Introduction

High-speed railway systems are being developed worldwide [1]. To keep the high travelling speed, trains have to move long distances in underground spaces of dense urban areas, tunnels in mountainous regions and across bays, harbours or rivers. Fire hazard in burning a train car should be carefully evaluated [2-4] in those underground or enclosed spaces. A big fire in open space is much easier to control, but the fire environment will be very hazardous in underground enclosed spaces.

Appropriate design fires [5] have to be agreed for fire hazard assessment in deep underground spaces, particularly long tunnels where firefighting is very difficult in comparing with open space. The heat release rate (HRR) is a key parameter in designing fire size of train cars and is related to factors such as train structure and material properties. It is not merely a variable used to characterize fire, it is the sole significant variable in defining the phenomenon of a fire hazard. The HRR is the driving force in developing a fire. Adverse effects, damage, and the quantity of combustion products increase with an increase in the HRR.

There has been some group discussion on train car fires in the Asia-Oceania areas [6-9] with rapid development of railway systems. A detailed review [10] of rail fire performance standards,

large train fire incidents, recent experiments on flashover train fires, surveys of design fires used in the past and existing design fire estimation methods were reported. Updated works on train car fires [11-17] are summarized. Design fire is a crucial and decisive parameter to predict room fire development in performance-based design on fire safety provisions.

Estimated HRR resulting from burning a train car from fire models can be used for designing adequate fire safety provisions [5-9] in underground stations and tunnels. There is concern on assuming a low design fire in subway stations and tunnels [9].

In this paper, HRR in a model train car CRH1 in China [18-20] will be studied as an example case to get a design fire for assessing fire hazards of train car in underground or enclosed spaces with a two-layer fire zone model computer program, the Consolidated Fire and Smoke Transport (CFAST) [21-24]. The computing time required is much shorter than Computational Fluid Dynamics (CFD) [25] models and appropriate for studying many fire scenarios, such as in studying cable fires in nuclear plants [26].

The radiative heat flux and temperature are used as the ignition criteria of combustibles to determine the HRR. The HRR of the seats of CRH1 measured in a full-scale fire test [19] will be used

for fire simulations. The ignition sequence of the burning train related to the peak point of the total HRR will be investigated. Simulated HRR of the train car will be compared with experimental HRR from full-scale burning tests in Japan, Korea and Sweden.

The HRR results will justify the design fire used for better high-speed train system fire safety. If the HRR of burning a train car is very high, current fire protection relying on the smoke management system [27,28] in the tunnel and underground stations might not be adequate.

Smoke extraction systems [5], either natural vents or mechanical ventilation, are installed to keep smoke layer at high levels in many big enclosed stations. A design fire with high HRR such as 20 MW is commonly used for designing natural vents, but a low HRR such as 5 MW is used for mechanical ventilation system. A sustainable new hybrid design combining the advantages of static and dynamic systems is proposed [29], which could result in a lower smoke temperature and higher smoke layer interface height, indicating a better extraction design.

Fire suppression system should be added if necessary. Water-based fire suppression [30] might be a solution in crowded deep underground spaces and long tunnels inside mountains or under water but more investigations have to be conducted.

2. The Model Train Car

The details of the example train car as reported by Chen et al. [18] are shown in Fig. 1a.

- Cars:

The length of the car is 26.95 m, the width is 3.328 m, and the height is 4.04 m.

- Windows:

The size of the windows is 1.9 m long and 0.6 m high. There are 20 windows in a second-class compartment train car, and the free distance between two windows is 1.9 m.

- Seats:

The number of seats is 101. The setting of seats is arranged as 2 and 3 on two sides. Seats are 0.45 m wide, the aisle is 0.58 m wide, and the free distance between two rows of seats is 0.45 m.

The oxygen consumption method [31] can be used to measure HRR accurately and reliably. Full-scale fire test of a double seat was reported by Zhu et al. [19] to determine the HRR of the seats. Four fire scenarios with two levels of ignition power and two ventilation rates were studied. The HRR data for the double seat under the four scenarios are displayed in Fig. 2.

3. Ignition

There are three basic modes of heat transfer in a fire [32]: conduction, convection and radiation. However, radiation is the dominant mode of heat transfer in the spread of flames within compartments. Combustible items away from a fire can be heated to ignition without direct flame contact. The spread of

fire between combustible items in the train car is primarily due to the thermal radiation from the burning source.

Similar findings were reported by Noordijk and Lemaire [33]. The flame propagates through radiation, depends on the quantity of heat released by 30-40%. Radiation heat transfer has the most significant impact on the spread of fire. When an object catches fire, the flame releases a large portion of the total released heat in the form of radiation. This radiation is then transmitted to other objects through the surrounding air. Other combustibles which absorb radiation would be heated up. Their temperature rises due to heating, and when their ignition temperature is exceeded, these components also begin to burn. Three different radiative processes involved are the emission of the radiation, the heat transfer through the air and the absorption of the radiation.

In this study, two parameters are used to determine ignition, the heat flux (Wm^{-2}) and temperature ($^{\circ}\text{C}$). Because the train car seats are a combination of various materials, their burning point is difficult to define accurately. Heat flux data from the National Fire Protection Association (NFPA) [34] and the ignition temperature of seats as determined by full-scale burning experiments [35] will be used.

4. Two Fire Scenarios

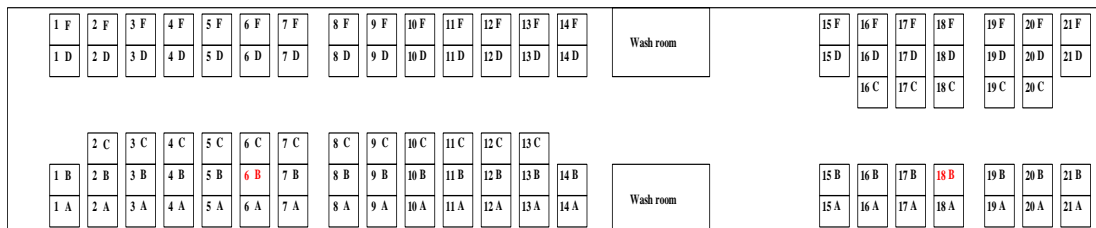
The position of the flame has a significant effect on the results of the heat flux measurement [36]. Two fire scenarios with different positions for the flame set in the train were considered as in Fig. 3.

- Scenario 1: Fire located in the front.
- Scenario 2: Fire in the rear.

The flame positioning for the two scenarios are shown also in Fig. 3a.

The first flame position modelled was in the middle of the front section. In the CFAST modelling, the first seat was assumed to have been ignited, and the HRR of the fire was defined by the full-scale burning test of the seat [19]. The targets of other seats were then placed around the burning seat and received the radiation of heat flux from the flame. Fig. 3b shows the setting of the CFAST simulation.

In the next process, the heat flux data from targets would be calculated by CFAST. According to the data, the time of heat flux to achieve 20 kWm^{-2} could be inferred. A 20 kWm^{-2} heat flux would initiate flashover in a residential room floor, according to NFPA921 [34]. In this simulation setting, the seats were assumed to be ignited when the heat flux achieved 20 kWm^{-2} . The ignition time of target seats was then input in CFAST, and the burning seats were defined as fires in the next burning process. These processes were repeated until the train car was burned out, and then the total HRR of the train car was calculated by CFAST. Fig. 3c shows the second ignition sequence for the first scenario.



(a) Layout of the example train car with seat numbers from Chen et al. [35]

1F (770s)	2F (765s)	3F (760s)	4F (755s)	5F (755s)	6F (750s)	7F (760s)
1D (770s)	2D (765s)	3D (760s)	4D (755s)	5D (745s)	6D (740s)	7D (750s)
	2C (765s)	3C (760s)	4C (755s)	5C (720s)	6C (440s)	7C (725s)
1B (770s)	2B (765s)	3B (760s)	4B (755s)	5B (710s)	6B (0s)	7B (715s)
1A (770s)	2A (765s)	3A (760s)	4A (755s)	5A (720s)	6A (440s)	7A (725s)
8F (765s)	9F (770s)	10F (1015s)	11F (1015s)	12F (1015s)	13F (1015s)	14F (1015s)
8D (765s)	9D (770s)	10D (1015s)	11D (1015s)	12D (1015s)	13D (1015s)	14D (1015s)
8C (760s)	9C (770s)	10C (1015s)	11C (1015s)	12C (1015s)	13C (1015s)	
8B (760s)	9B (770s)	10B (1015s)	11B (1015s)	12B (1015s)	13B (1015s)	14B (1015s)
8A (760s)	9A (770s)	10A (1015s)	11A (1015s)	12A (1015s)	13A (1015s)	14A (1015s)
15F (1045s)	16F (1045s)	17F (1045s)	18F (1045s)	19F (1045s)	20F (1045s)	21F (1045s)
15D (1045s)	16D (1045s)	17D (1045s)	18D (1045s)	19D (1045s)	20D (1045s)	21D (1045s)
	16C (1045s)	17C (1045s)	18C (1045s)	19C (1045s)	20C (1045s)	
15B (1045s)	16B (1045s)	17B (1045s)	18B (1045s)	19B (1045s)	20B (1045s)	21B (1045s)
15A (1045s)	16A (1045s)	17A (1045s)	18A (1045s)	19A (1045s)	20A (1045s)	21A (1045s)

(b) Time to ignition at each car seat for Scenario 1

1F (1500s)	2F (1500s)	3F (1500s)	4F (1500s)	5F (1500s)	6F (1500s)	7F (1500s)
1D (1500s)	2D (1500s)	3D (1500s)	4D (1500s)	5D (1500s)	6D (1500s)	7D (1500s)
	2C (1500s)	3C (1500s)	4C (1500s)	5C (1500s)	6C (1500s)	7C (1500s)
1B (1500s)	2B (1500s)	3B (1500s)	4B (1500s)	5B (1500s)	6B (1500s)	7B (1500s)
1A (1500s)	2A (1500s)	3A (1500s)	4A (1500s)	5A (1500s)	6A (1500s)	7A (1500s)
8F (1500s)	9F (1500s)	10F (1465s)	11F (1465s)	12F (1465s)	13F (1465s)	14F (1465s)
8D (1500s)	9D (1500s)	10D (1465s)	11D (1465s)	12D (1465s)	13D (1465s)	14D (1465s)
8C (1500s)	9C (1500s)	10C (1465s)	11C (1465s)	12C (1465s)	13C (1465s)	
8B (1500s)	9B (1500s)	10B (1465s)	11B (1465s)	12B (1465s)	13B (1465s)	14B (1465s)
8A (1500s)	9A (1500s)	10A (1465s)	11A (1465s)	12A (1465s)	13A (1465s)	14A (1465s)
15F (1150s)	16F (1180s)	17F (1170s)	18F (1170s)	19F (1170s)	20F (1175s)	21F (1180s)
15D (1150s)	16D (1170s)	17D (1160s)	18D (1160s)	19D (1170s)	20D (1175s)	21D (1180s)
	16C (1150s)	17C (1140s)	18C (1150s)	19C (1170s)	20C (1175s)	
15B (1140s)	16B (1130s)	17B (800s)	18B (0s)	19B (1170s)	20B (1175s)	21B (1180s)
15A (1140s)	16A (1130s)	17A (780s)	18A (390s)	19A (1170s)	20A (1175s)	21A (1180s)

(c) Time to ignition at each car seat for Scenario 2

Fig. 1. Example train car model

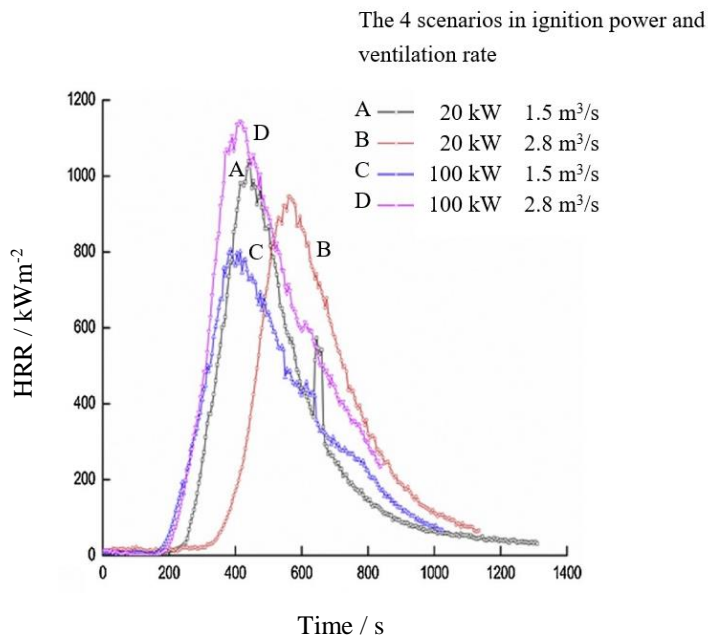
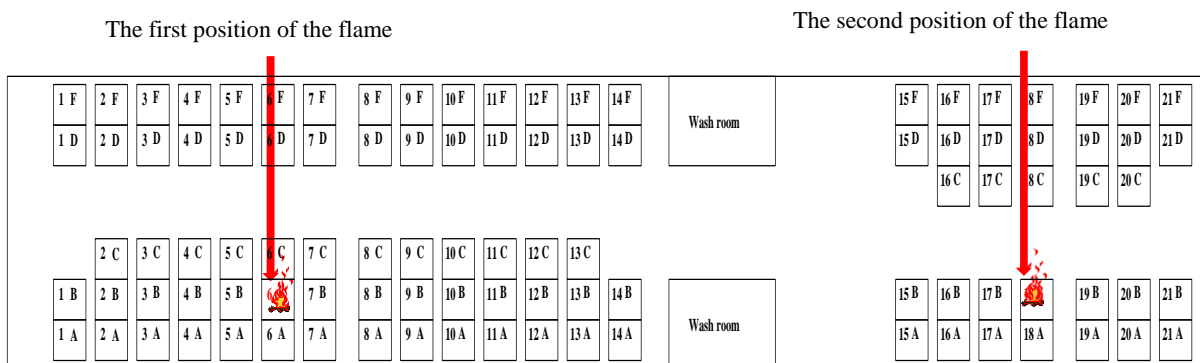
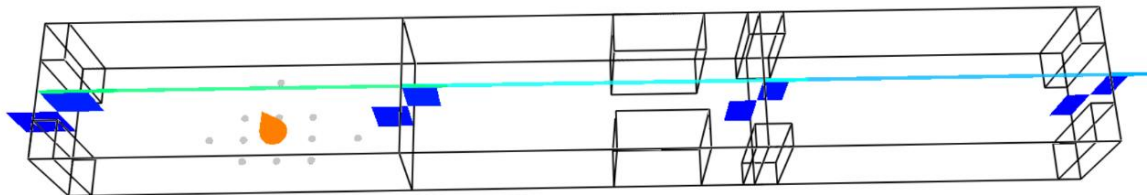


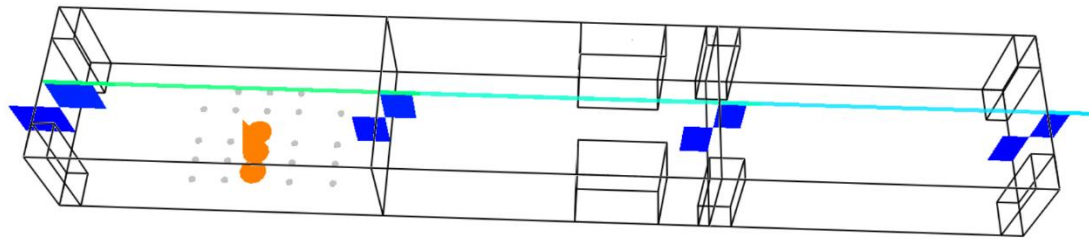
Fig. 2. HRR of double seat by Zhu et al. [19]



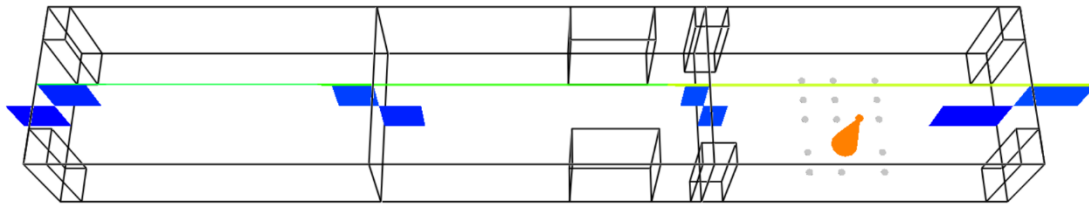
(a) Positions of ignition in the example train car model



(b) The first position of flame and targets



(c) The second ignition sequence for scenario 1



(d) The second position of flame and targets for scenario 2

Fig. 3. The train model simulation

The CRH1 train car has two washing rooms and luggage racks near the middle to separate the car into two sections. The number of seats in the front section of the train car is greater than the number in the rear section. The aisle between the washing rooms would affect the heat transfer and the ignition sequence of the burning test. Therefore, it was essential to also set up a second scenario in which a fire started in the rear portion of the car.

The flame position for the second scenario was in the middle of the rear section of the train car. The arrangement of seats in the rear differs from that in the front: the positions of the double and triple seats are swapped. In addition, the total number of seats in the rear portion is only 33, fewer than the 68 seats in the front section. In scenario 2, the HRR of the first ignited seat was also defined using data from the full-scale burning test of the seat from Zhu et al. [19]. Next, additional seats were placed around the burning seat as targets and received the radiation of heat flux from the flame. Fig. 3d shows the set-up of the second experiment in scenario 2 in CFAST.

The subsequent experimental steps from scenario 1 were then repeated with the scenario 2 set-up until the entire car was burned out. Finally, the final HRR data for the scenario 2 experiments were calculated and recorded.

The ventilation condition is one of the two primary factors determining the HRR, the other factor being the fire load [11]. During a fire in a passenger train car, ventilation conditions, such as the number and location of windows, directly determine the HRR and air supply in the passenger car, because the internal space of the car is minimal, and the fire load is usually relatively fixed.

Chen et al. [35] tested different ventilation conditions in a train car using CFD. They assumed various scenario conditions, including that the door in the middle of the car would be opened, and that the windows would be broken when the HRR of the fire reached the setting points. These assumptions are controversial because when a fire occurs in a running train, the passengers' first choice is to escape to a car that is not on fire.

Therefore, the ventilation setting for this experiment assumed that the doors in the middle of the train car and the windows were closed. The doors connecting the two train cars would remain open, so the doors were set open to the outside environment in the CFAST ventilation setting.

The experimental results of burning seats provide a large amount of data. These data are best viewed and compared graphically. In accordance with the aim of this research, the primary interest is the HRR, which is influenced by the ignition sequence of the seats, and this ignition sequence, in turn, is determined by the radiant heat flux of the seats. Therefore, the analysis is almost entirely related to the radiant heat flux, the ignition sequence and the HRR. Thus other measures, such as temperature, will not be presented here.

In order to clearly illustrate the results of the simulation experiment, the position of each seat is marked with a number, as shown in Fig. 1a. Predicted ignition time at each seat will be shown later.

5. Results on Scenario 1

5.1 Target Heat Flux

In scenario 1, three ignition sequences were required in the model to ignite the entire train car. The heat flux of targets surrounding the fire in three ignition sequences are as follows:

After the seat 6B was ignited, the heat flux of surrounding seats 6A and 6C reached 20 kWm^{-2} as in Fig. 4a. As described in section 3.5, seats 6A and 6C were ignited by the radiation from 6B. Fig. 4b shows the heat flux surrounding the three burning seats (6A, 6B and 6C).

In the case in which three seats were ignited, the seats' radiant heat flux in the front nine rows of the car exceeded 20 kWm^{-2} . The heat flux of the seats near the fire source even reached 40 kWm^{-2} . In the second ignition sequence, nine rows of seats, almost half of the seats in the train car, were ignited. Fig. 4c shows the heat flux of other seats behind the front nine rows of burning seats.

Under this condition, the train car was flashover by radiation. All seats in the car were ignited, and the heat flux of the radiation reached a peak of almost 550 kWm^{-2} .

5.2 Time to Ignition

The modelled heat flux was described above with comparisons displayed in line charts. The accurate time to ignition for each seat in scenario 1 is shown in Fig. 1b.

Based on the time to ignition of the train car seats, the flashover might occur between 1,015 s and 1,045 s after the initial

fire source was ignited. By this point, more than half of the seats would have been ignited, and they would release a great deal of heat by this point in time.

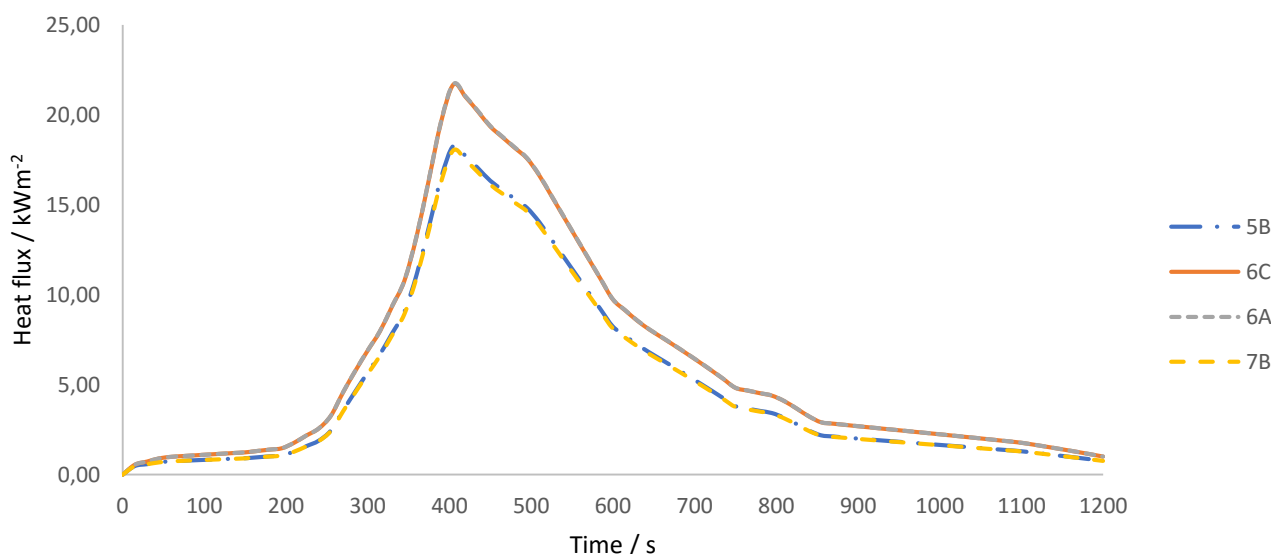
5.3 Heat Release Rate

The HRR of a single seat was determined from a full-scale burning test. Fig. 5 shows the HRR of a seat, which was input into the CFAST model as the core data for the simulations.

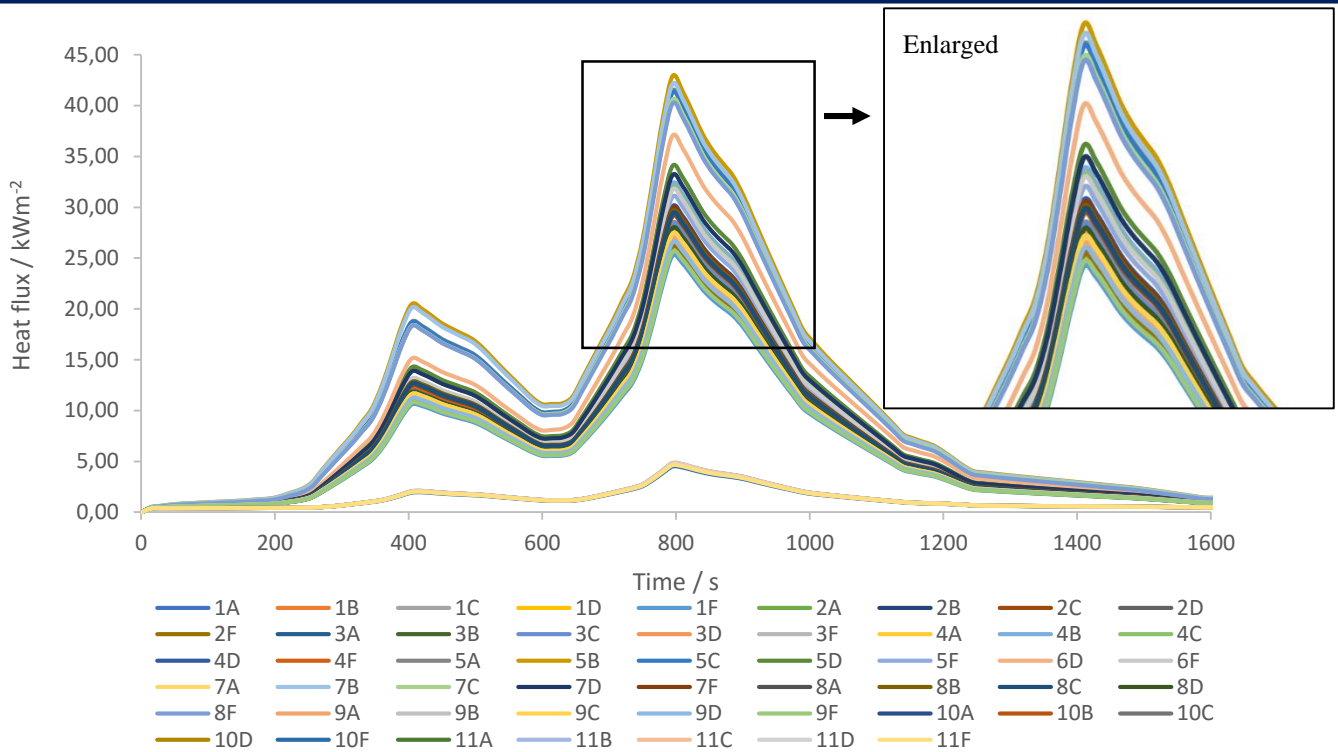
Fig. 6a shows the HRR of the first ignition sequence in scenario 1. During this sequence, three seats burned: seat 6B was ignited at the start, and seats 6A and 6C ignited at the 440-s mark.

In the second ignition sequence in scenario 1, the front nine rows of seats ignited, and the total number of burning seats reached 44. Removing those three seats (6A, 6B and 6C) that had been already ignited in the first ignition sequence leaves 44 seats ignited during the second ignition sequence. The ignition time of these seats was between 710 s and 770 s, with the specific timing for each seat determined by its proximity to the fire source of those three burning seats. The simulation results demonstrated that the HRR peaked at 25 MW, a peak that lasted for about 300 s. Fig. 6b shows the HRR curve of the scenario 1 second ignition sequence.

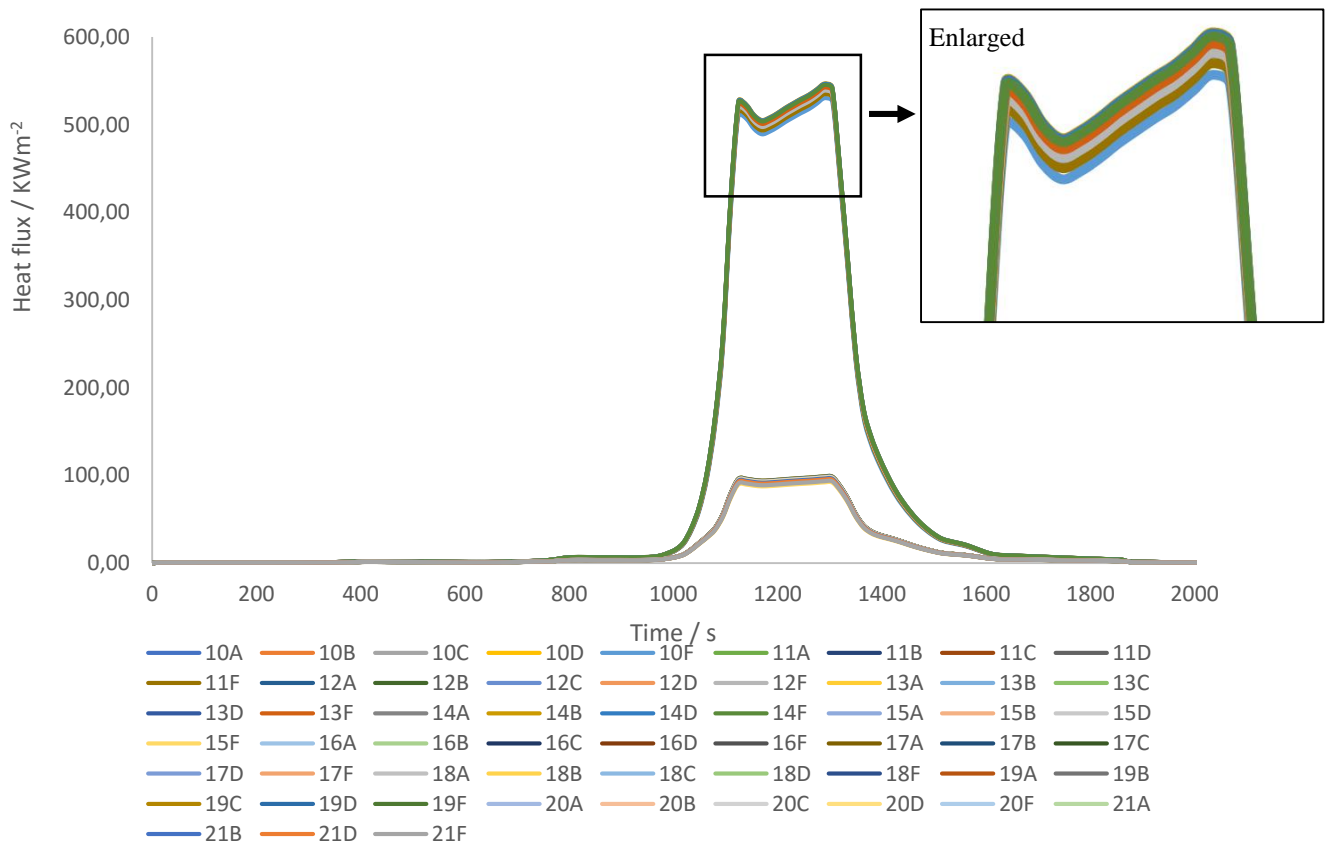
In the third ignition sequence, flashover occurred, and the remaining seats in the train car were ignited in a short period of time. The HRR increased rapidly at 1,000 s and peaked at approximately 40 MW at 1,400 s. Fig. 7 shows the overall HRR curve of the train car fire in scenario 1.



(a) 4 seats surrounding the burning seat 6B



(b) 11 seats surrounding the burning seats 6A, 6B and 6C



(c) 12 rows seats at rear behind the burning seats in front rows 1 to 9

Fig. 4. Scenario 1: The heat flux of seats

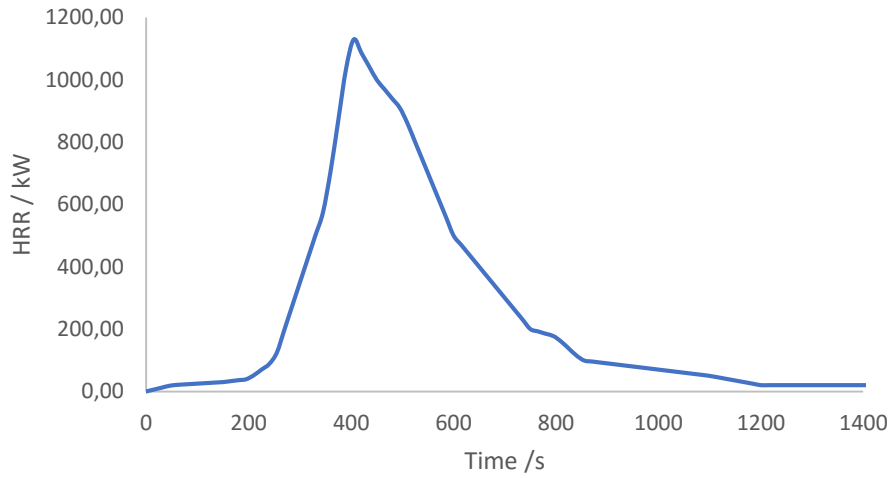
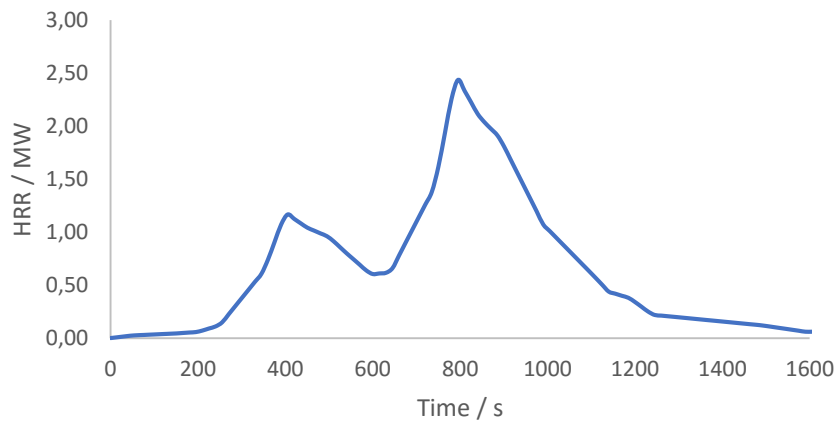
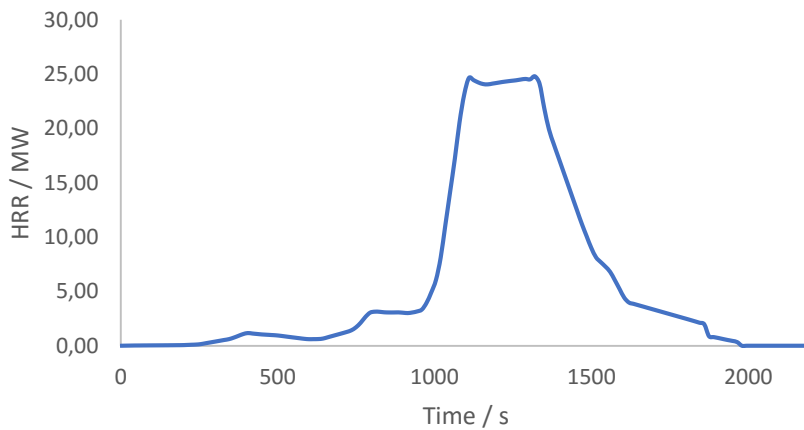


Fig. 5. The HRR of a single seat (Zhu et al. [19])



(a) The first ignition sequence



(b) The second ignition sequence

Fig. 6. HRR for Scenario 1

6. Results on Scenario 2

6.1 Target Heat Flux

In scenario 2, the model used four ignition sequences to ignite the entire train car. The heat flux of target seats surrounding the fire in the four ignition sequences are shown in the following:

After the seat 18B was ignited, surrounding seats in three rows (the 17th, 18th and 19th rows) were set as targets to measure the heat flux. From the results in Fig. 8a, it can be seen that the heat flux of seat 18A, immediately next to burning seat 18B, reached 20 kWm^{-2} . In the next ignition sequence, these two seats were assumed to be ignited. Fig. 8b shows the heat flux for the five rows of seats surrounding these two burning seats.

The outcome of the second ignition sequence in scenario 2 differed from that seen in scenario 1. In this case, only two additional seats (17A and 17B) were ignited by the radiation heat

flux of the two burning seats. Compared to scenario 1, the size of the fire in the third ignition sequence was smaller in scenario 2. Fig. 8c shows the heat flux data for the third ignition sequence in scenario 2.

The results of the third ignition sequence indicated that the rear section of the train car was fully ignited, because the heat flux for all seats reached 20 kWm^{-2} . Fig. 9 displays the fourth ignition sequence for Scenario 2, with all seats in the rear section of the train car burning.

In scenario 2, the train car fire model required four ignition sequences to spread and ignite 101 seats. At the same time, it showed that the position of the incident fire source would affect the result and progress of the train car fire.

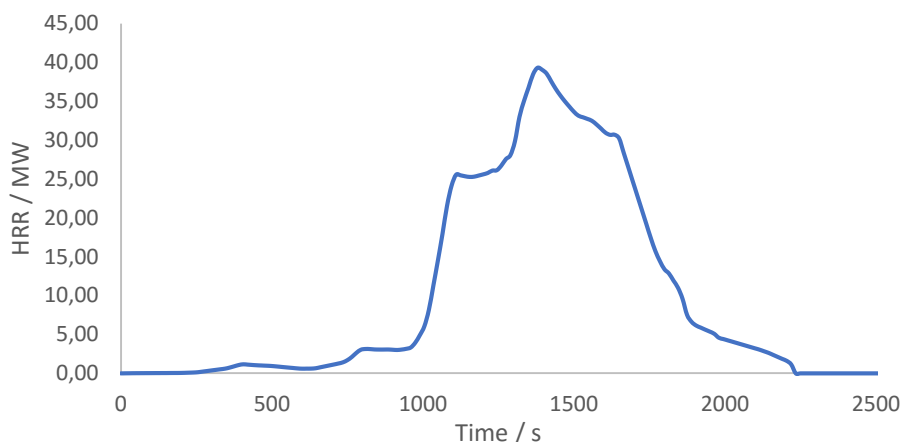
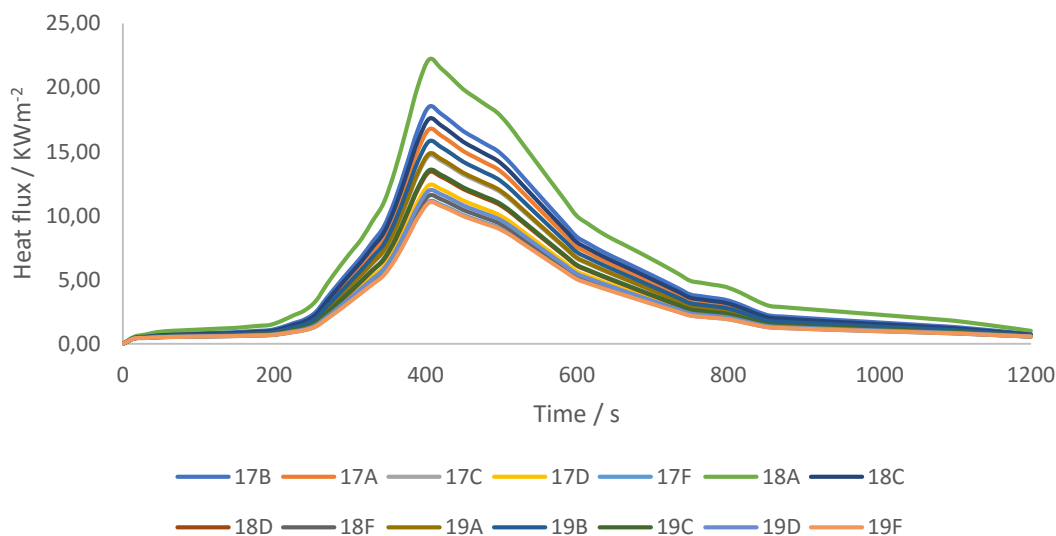
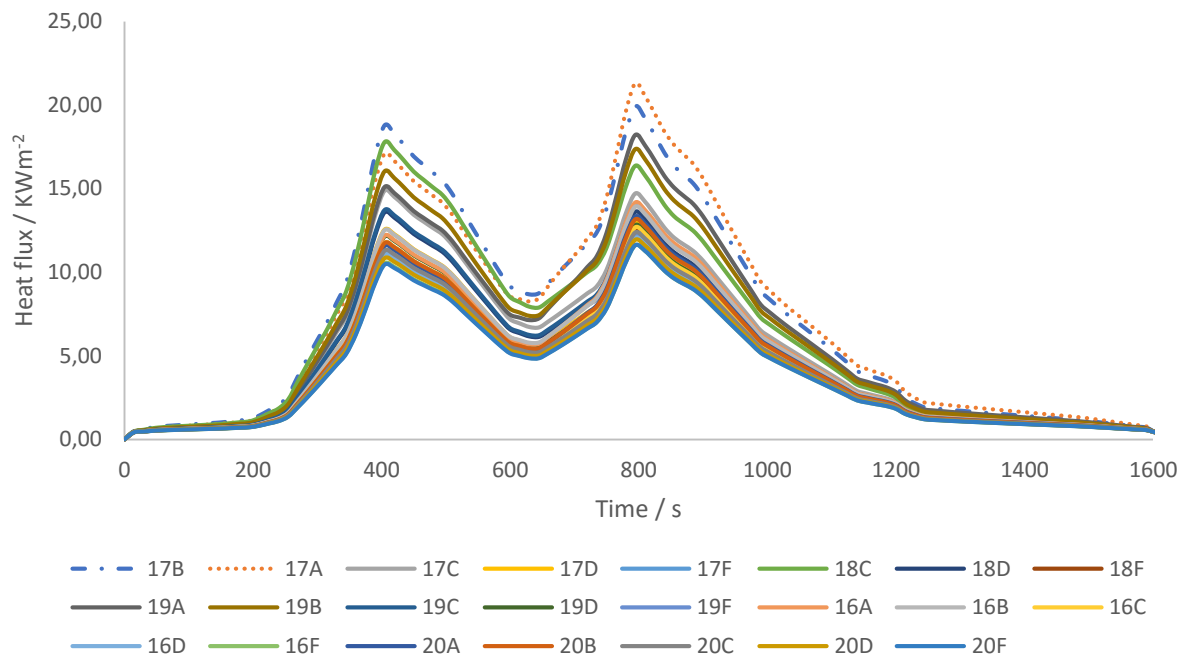


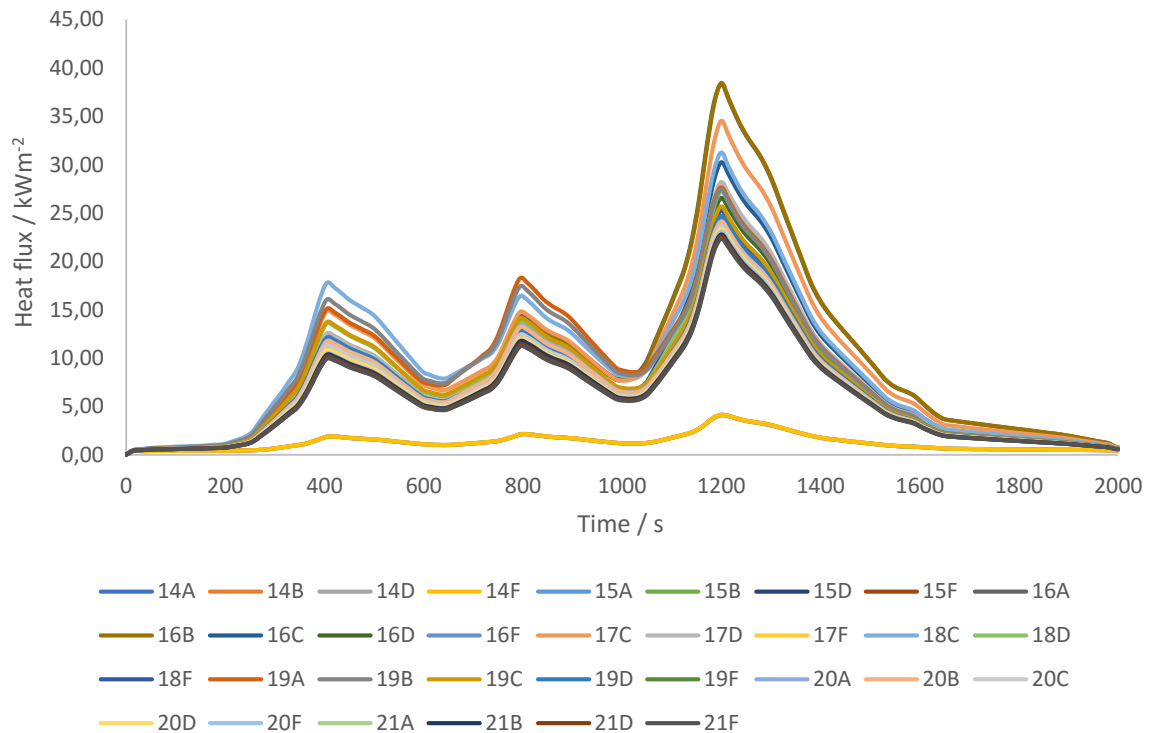
Fig. 7. HRR of the train car in scenario 1



(a) 3 seats surrounding the burning seat 18B

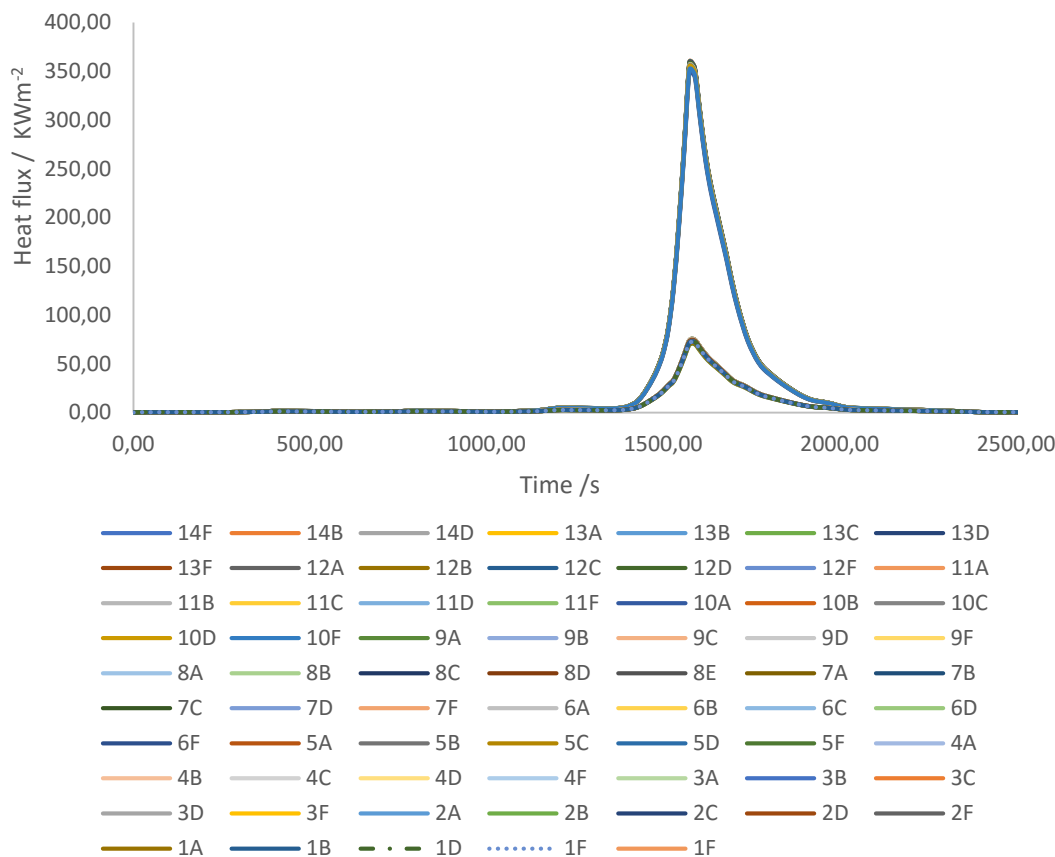


(b) 5 seats surrounding burning seats 18A and 18B



(c) 8 rows seats burning seats 17A, 17B, 18A and 18B

Fig. 8. Scenario 2: The heat flux of seats



(14 rows seats in the front half of train car)

Fig. 9. The heat flux of the front section of the train car

6.2 Time to Ignition

The time to ignition for each seat in scenario 2 is shown in Fig. 1c. The position of the first ignited seat in scenario 2 differed from that used in scenario 1.

Compared to the time to ignition results from scenario 1, the flashover in scenario 2 would be delayed by about 450 seconds, occurring between 1,465 s and 1,500 s after the initial seat had been ignited. About two-third of the seats would have been ignited by this time, resulting in a higher HRR in scenario 2 than scenario 1. The next section addresses the HRR for these two scenarios.

6.3 Heat Release Rate

Scenario 2 differed in that the first burning seat (18B) was in the rear section of the train car, and this change in source position of the fire led to a different ignition sequence and HRR. There were four ignition sequences in scenario 2.

In the first ignition sequence, the seat 18B was ignited. The second seat (18A) was ignited at 390 s. Because only two seats were burning, the HRR was lower than that for the first sequence

in scenario 1. Fig. 10a shows the HRR of the first ignition sequence in scenario 2.

Only four seats were ignited during the second ignition sequence in scenario 2, compared with 44 seats that were burning in the same sequence in scenario 1. The HRR of the second ignition sequence in this scenario had three peaks, with the maximum peak less than 2.5 MW. Fig. 10b shows the HRR curve of the second ignition sequence.

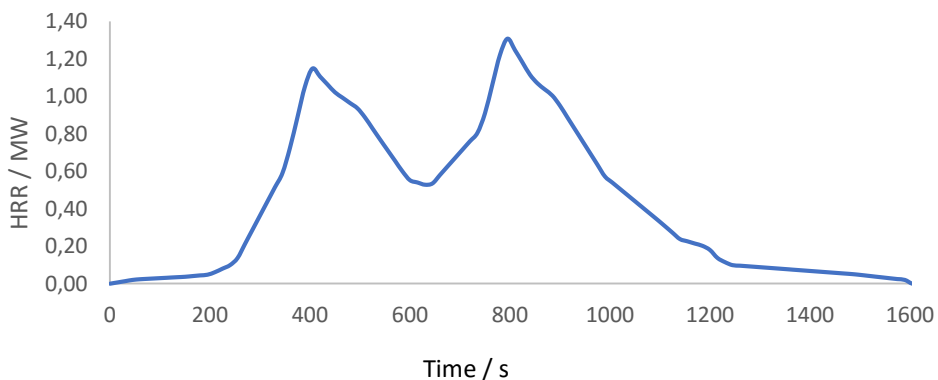
During the third ignition sequence in scenario 2, all seats in the rear section of the train car were ignited, for a total of 33 burning seats. The 29 newly ignited seats were burning during the short span from 1,130 s to 1,180 s. The total HRR of these seats was extremely high and exceeded 30 MW at 1,550 s. Fig. 10c shows the HRR of the third ignition sequence.

In the fourth ignition sequence, the extremely high HRR of the rear section of the train car ignited the remaining seats in the front section. The flashover occurred at 1,700 s, and the HRR peaked at 43 MW. Compared with the final HRR (almost 40 MW) and the total burning time (2,200 s) in scenario 1, the HRR

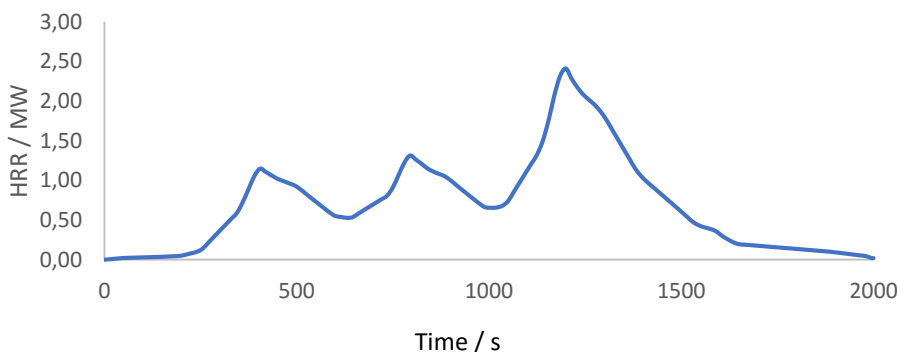
in scenario 2 was greater, and the burning lasted longer. Fig. 11 shows the total HRR curve of the train car in scenario 2.

A good review of HRR train car was reported [10]. There are detailed descriptions on full-scale burning tests of train cars conducted in Sweden [17] and South Korea [17]. The heat release

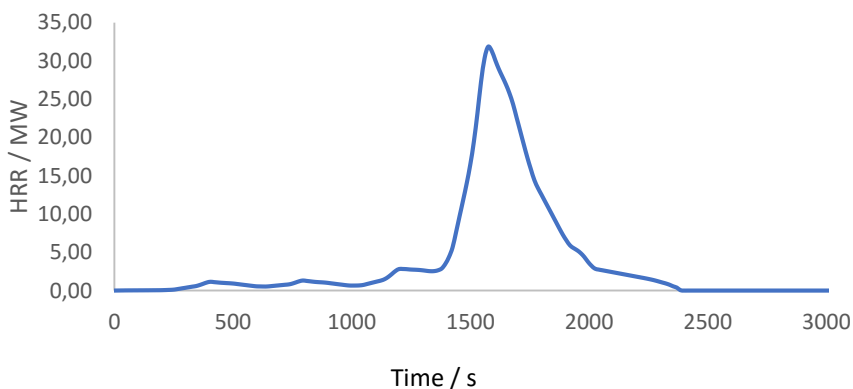
rates measured from experimental oxygen consumption method are shown in Figs. 12a and 12b respectively. Results of the present simulation by zone models CFAST are very close to those overseas studies in Fig. 12.



(a) The first ignition sequence



(b) The second ignition sequence



(c) The third ignition sequence

Fig. 10. HRR for Scenario 2

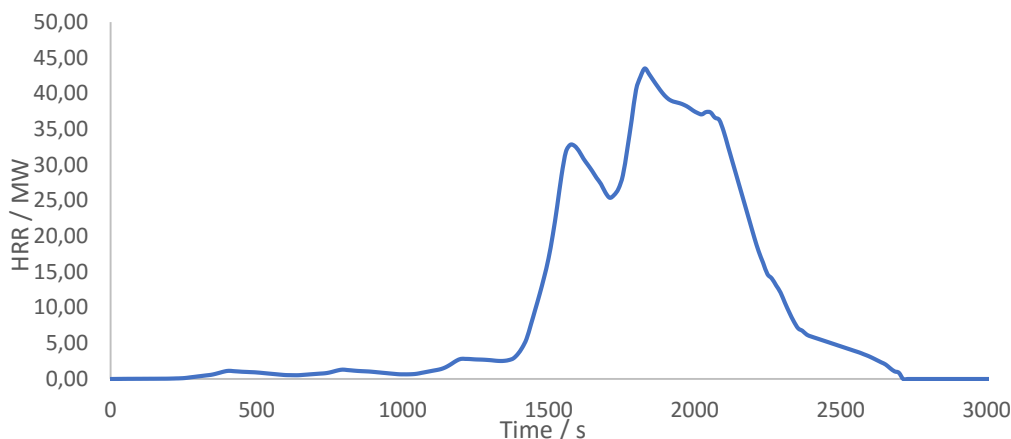
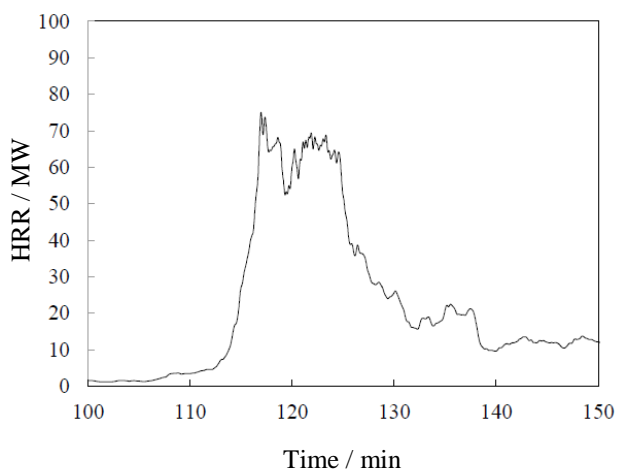
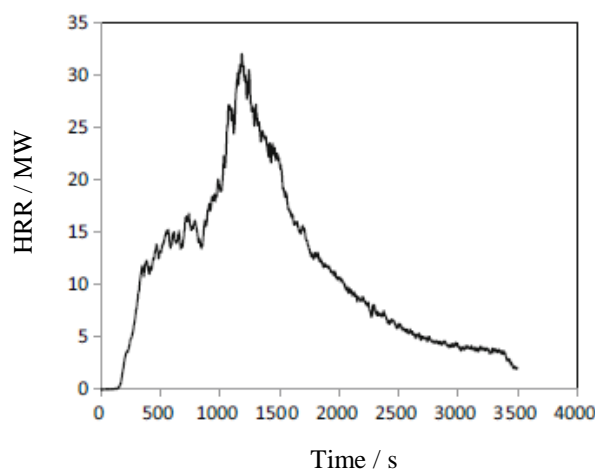


Fig. 11. HRR of the train car in scenario 2



(a) Sweden (Lönnermark et al. [14])



(b) Korea (Lee et al. [17])

Fig. 12. HRR of train car measured overseas

7. Conclusions

Design fire for fire hazard assessment in underground spaces in a burning CRH1 example train car was studied by fire simulation with experimental data from a full-scale burning test of seats. Similar studies can be carried out for another train car model. The heat flux of 20 kWm^{-2} and the temperature of 370°C were used as the ignition criteria for the fire zone model CFAST. The HRR data from the simulation software were compared with the HRR data from full-scale burning tests of a train car conducted in Sweden and South Korea. The results illustrated that the HRR data generated by CFAST are relatively close to the HRR data obtained from the actual full-scale burning test. Moreover, from the data analysis of the CRH1 train car with only the seat being combustible, the HRR of the CRH1 train is

close to the HRR of other train cars containing more combustibles including baggage and curtains, so the fire load and the HRR of the actual CRH1 train car will be even higher.

- The simulation used the most extreme setting, using 20 kWm^{-2} of heat flux as the seat’s ignition setting. According to data from experiment, it can be inferred that the seat may be ignited at a certain time after receiving a heat flux of less than 20 kWm^{-2} . Therefore, the burning rate of the actual CRH1 train car is higher than the experimental results.
- By using CFAST in the simulation, upon igniting the first seat, it is not necessary to add the igniting fire source in the simulations. This makes CFAST a powerful tool in simulating fire spreading.
- The position of initial seat ignition has significant effect on fire spreading and HRR.

Based on these conclusions, to improve the intrinsic safety of burning train car inside deep underground spaces or long tunnels, CRH1 designers should consider reducing HRR. Amount of flammable materials should be limited so as not to give a high fire load in train design in order not to give hazards to underground spaces or tunnels. In particular, upgrading of the current seats should be considered. To better protect the personal safety of passengers, they should consider the addition of flame-retardant fireproof panels dividing the compartment into three to four fire zones, which will delay fire spread rate to allow passengers having longer escape times.

The data in the present study can also be used to design the future CRH1-type of train car with lower HRR to ensure the safety of future experimental personnel and equipment.

As the HRR of burning a train car can be very high, current fire protection which relies on the smoke management system in the tunnel and underground stations might not be adequate. Water fire suppression might be a solution but more investigations have to be conducted.

Acknowledgement

The work described in this paper was supported by a grant from the Research Grants Council of the Hong Kong Special Administrative Region, China for the project "Safety, Reliability, and Disruption Management of High Speed Rail and Metro Systems" (Project No. T32-101/15-R) with account number 3-RBAC".

Conflict of Interest Statement

The authors declare that there is no conflict of interest in the study.

CRediT Author Statement

W.C. Xiao: Conceptualization, Investigation, Formal analysis, Visualization, Writing-original draft,

W.K. Chow: Conceptualization, Investigation, Resources, Writing-original draft, Writing-review and editing, Supervision,

W. Peng: Formal analysis, Validation, Visualization, Writing-original draft.

References

- [1] Lo TY. Reactivating high-speed railway systems between Singapore and Laos. *Yazhou Zhoukan*, 2022; Issue 50, Cover Feature (In Chinese).
- [2] Chow WK. A discussion on estimating the heat release rate of design fires in Hong Kong. *J Applied Fire Sci*. 2012-2013; 22(2), 143-149.
- [3] Chow WK. Several points to watch on fire hazards of railway systems. The 4th Workshop on Railway Operation for Safety and Reliability (Special session of IEEE Global Reliability and Prognostics & Health Management Conference, PHM-2020, 16-18 October 2020, Shanghai, China), Organized by City University of Hong Kong, Hong Kong, 17 October 2020.
- [4] Pardhi S, Deshmukh A, Ajrouche H. Modelling and simulation of detailed vehicle dynamics for development of innovative power-trains. *Int J Automot Sci Technol*. 2021; 5(3), 244-253.
- [5] Qu L, Chow WK. Common practices in fire hazard assessment for underground transport stations. *Tunnelling Underground Space Technol*. 2013; 38, 377-384.
- [6] Proceedings of 2011 Exchange Meeting for SFPE Asia-Oceania Chapters – Transportation Fire Safety, Korea Railroad Research Institute & SFPE Korean Chapter, Seoul, Korea, 28 April 2011.
- [7] Lattimer B, Beyler C. Heat release rates of fully-developed fires in railcars. *Fire Safety Science – Proceedings of the Eighth International Symposium*, 2005, pp. 1169-1180.
- [8] Dowling VP, White N, Webb AK, Barnett JR. When a passenger train burns, how big is the fire? *Proceedings of the 7th Asia-Oceania Symposium on Fire Science and Technology*, pp. 19-28, Hong Kong, September 2007.
- [9] Chow WK. Safety to watch in crowded railway systems. *Asia-Oceania SFPE Chapters Conference*, Jakarta, Indonesia, 29 May 2015.
- [10] White N. Fire performance of passenger trains. *Fire Australia*, 1 January 2017.
- [11] Ingason H. Model scale railcar fire tests. *Fire Saf. J*. 2007; 42, 271-282.
- [12] Ko YJ, Michels R, Hadjisophocleous GV. Instrumentation design for HRR measurements in a large-scale fire facility. *Fire Technol*. 2011; 47, 1047-1061.
- [13] Schebel K, Meacham BJ, Dembsey NA, Johann M, Tubbs J, Alston J. Fire growth simulation in passenger rail vehicles using a simplified flame spread model for integration with CFD analysis. *J Fire Protect Eng*. 2012; 22(3), 197-225.
- [14] Lönnermark A, Claesson A, Lindström J, Li YZ, Kumm M, Ingason H. Full-scale fire tests with a commuter train in a tunnel. *SP Technical Research Institute of Sweden*, SP Report: 2012.05.
- [15] Capote JA, Jimenez JA, Alvear D, Alvarez J, Abreu O, Lazaro M. Assessment of fire behaviour of high-speed trains' interior materials: small-scale and full-scale fire tests. *Fire Mater*. 2014; 38, 725-743.
- [16] Zicherman J, Lautenberger C, Wolski A. Challenges in establishing design fires for passenger rail vehicles. *Fire and Materials 2015 Conference*, 2-4 February 2015, San Francisco, USA.
- [17] Lee D, Park WH, Hwang JH, Hadjisophocleous G. Full-scale fire test of an intercity train car. *Fire Technol*. 2016; 52(5), 1559-1574.
- [18] Chen JM, Yao XL, Yan G, Guo XH. Comparative study on heat release rate of high-speed passenger train compartments. *J Procedia Eng*. 2014; 71, 107-113.
- [19] Zhu J, Li XJ, Cheng FM. Combustion performance of flame-ignited high-speed train curtains via full-scale tests. *Journal of Railway Science and Engineering*, 2015; Issue 2, 257-263.
- [20] Li ZG, Li ZQ, Liu WM. Study on the calculation methods of high-speed train heat release rate. *Railway Locomotive and Car*, 2018; 01-0015-04. (In Chinese)
- [21] Peacock RD. *CFAST Volume 4: Software Quality Assurance*. National Institute of Standards and Technology, USA, 2018.

- [22] Peacock RD, McGrattan K.B, Forney GP, Reneke PA. CFAST Volume 1: Technical Reference Guide. National Institute of Standards and Technology, USA, 2018.
- [23] Peacock RD, Reneke PA, Forney GP. CFAST Volume 2: User's Guide. National Institute of Standards and Technology, USA, 2018.
- [24] Peacock RD, Reneke PA, Forney GP. CFAST Volume 3: Verification and Validation Guide. National Institute of Standards and Technology, USA, 2018.
- [25] McGrattan K, Hostikka S, McDermott R, Floyd J, Weinschenk C, Overholt K. Fire Dynamics Simulator, User's Guide. NIST Special Publication 1019, Sixth Edition. National Institute of Standards and Technology, Gaithersburg, Maryland, USA, and VTT Technical Research Center of Finland, Espoo, Finland, November 2013.
- [26] Huang X, Ren Z, Zhu H, Peng L, Cheng CH, Chow WK. A modified zone model on vertical cable tray fire in a confined compartment in the nuclear power plant. *J Fire Sci.*2018; 36(6), 472-493.
- [27] Hong Kong Airport Authority. Hong Kong International Airport Tenant Design Guideline, Appendix A Sample Fire Engineering Report, April 2011 version, Issue no. 3, 2011.
- [28] Buildings Department. Code of Practice for Fire Safety in Buildings 2011 (October 2015 version). The Hong Kong Special Administrative Region.
- [29] Ivanov M, Peng W, Wang Q, Chow WK. Sustainable smoke extraction system for atrium: A numerical study. *Sustainability*, 2021; 13(13): 7406.
- [30] Li J, Li YF, Bi Q, Li Y, Chow WK, Cheng CH, To CW, Chow CL. Performance evaluation on fixed water-based firefighting system in suppressing large fire in urban tunnels. *Tunnelling Under-ground Space Technol.* 2019; 84, 56-69.
- [31] Chow WK, Han SS. Heat release rate calculation in oxygen consumption calorimetry. *J Appl Therm Eng.* 2011; 31, 304-310.
- [32] Fleury R, Spearpoint M, Fleischmann C. Evaluation of thermal radiation models for fire spread between objects. University of Canterbury, Department of Civil and Natural Resources Engineering, 2010.
- [33] Noordijk L, Lemaire T. Modelling of fire spread in car parks. *HERON*, 2005; 50(4), 209-218.
- [34] National Fire Protection Association. NFPA 921, Guide for Fire and Explosion Investigations, National Fire Protection Association, USA, 2004.
- [35] Chen JM, Yao XL, Li SP. Study on the influence of ventilation condition on the heat release rate of the CRH passenger rail car. *J Procedia Eng.* 2013; 62, 1050-1056.
- [36] Lönnermark A, Ingason H. Fire spread between industry premises. *Fire Safety Science – Proceedings of the 10th IAFSS Symposium*, 2011; pp. 1305-1317.